

Research on Effect of Icing Degree on Performance of NACA4412 Airfoil Wind Turbine

Yuhao Jia¹, Bin Cheng^{1,2,*}, Xiyang Li^{1,2}, Hui Zhang^{1,2} and Yinglong Dong¹

¹College of Mechanical and Electrical Engineering, Shihezi University, Shihezi, 832003, China

²Key Laboratory of Northwest Agricultural Equipment, Ministry of Agriculture and Rural Affairs, Shihezi, 832003, China

*Corresponding Author: Bin Cheng. Email: cb_adu@shzu.edu.cn

Received: 11 June 2020; Accepted: 07 July 2020

Abstract: In order to study the effect of icing on the wind turbine blade tip speed ratio and wind energy utilization coefficient under working conditions, it is important to better understand the growth characteristics of wind turbine blade icing under natural conditions. In this paper, the icing test of the NACA4412 airfoil wind turbine was carried out using the natural low temperature wind turbine icing test system. An evaluation model of icing degree was established, and the influence of wind speed and icing degree on the performance parameters of wind turbines was compared and analyzed. It is shown that icing is mainly concentrated on the leading edge of the blade and the windward side. The icing on the leeward surface is concentrated near the leading edge of the blade. The amount of icing varies significantly along the direction of blade expansion, with the least amount of ice accumulation at 0.2R, followed by 0.6R, and most at 0.95R. At the beginning of the experiment, the icy thickness at the 0.2R, 0.6R and 0.95R locations increased at a rate of 12.03%, 8.87% and 6.00% respectively, and then the growth rate gradually decreased and stabilized. At the same wind speed, the blade tip speed ratio and wind energy utilization coefficient are inversely related to the change trend of the icing degree. When the blade icing degree is 0.82%, 1.49% and 2.73%, the maximum tip speed ratio is reduced by 7.1%, 14.1% and 21.2% and the maximum wind energy utilization coefficient is reduced by 36.3%, 51.2% and 61.6% respectively.

Keywords: Wind turbine; blade icing; icing degree; blade tip speed ratio; wind energy utilization coefficient

1 Introduction

The wind energy storage in the high and cold areas is huge, and the density of cold air is large, and wind power equipment can generate more electrical energy. Due to the low population density, wind power projects in cold regions have more room for development [1]. However, wind turbines in these areas are often operated under conditions that are prone to freezing in the atmosphere, which has a detrimental effect on wind turbine performance. As a result, the development of wind power generation technology in cold regions is severely restricted. Wind turbine ice accumulation caused changes in blade structure



This work is licensed under a Creative Commons Attribution 4.0 International License, which permits unrestricted use, distribution, and reproduction in any medium, provided the original work is properly cited.

parameters and surface roughness, which reduced its inherent airfoil aerodynamic characteristics. The resulting blade stall may be advanced or delayed, leading to severe wind turbine power loss [2].

Researches on wind turbine blade ice accumulation mainly include experimental research and numerical simulation. Due to the large size of wind turbines, scaled blade models are often used in experimental research. Janusz [3] used a combination of experiments and numerical calculations to simulate the flow of super-cooled water droplets on the blades through the Euler method two-dimensional flow model. The test computations were performed for the NACA 23012 airfoil, for two cases of droplet diameter and droplet phase concentration. The comparisons demonstrate close agreement of the computed results (mass of captured water in unit time, surface distribution and local maximum value) for low values of Liquid Water Content, defined in FAR25 airworthiness regulations. Shu et al. [4] used the 3D rotating flow field to calculate the ice accumulation of wind turbine blades, and obtained the conclusion that the blade ice type is glazed ice. Han et al. [5] conducted icing experiments using small wind turbine blades. The effects of different conditions such as liquid water content, freezing temperature and angle of attack on the ice shape were studied. Han used LEWICE software developed by NASA to simulate blade ice accumulation. The results show that the LEWICE simulation results are in good agreement with the experimental results under frost and ice conditions. However, the calculation results under glaze ice conditions are quite different.

Kasper [6] simulated the ice accumulation on the leading edge of the fan blade. It is proposed that glaze ice has the most serious effect on aerodynamic performance of the blade. However, only numerical simulation studies have been conducted, and no experimental verification has been conducted. Hochart et al. [7] used NACA airfoil for ice accretion research. It is concluded that icing of wind turbine blades deteriorates the aerodynamic performance of the airfoil. Only one different position in the radial direction of the blade was selected during the study. No icing experiment was conducted on the wind turbine in working condition. Wang et al. [8] studied the reduction of wind turbine power loss and speed reduction under different icing thicknesses. Tahere et al. [9] considered the uncertainty caused by wind turbine ice accumulation, and introduced a robust control mode through simulation. This mode can control the pitch angle and improve the performance of the wind turbine. The above literature analyzes the effect of icing on aerodynamic performance of the blade airfoil and the output power and speed of the wind turbine. However, it does not deeply study the effect of ice accumulation on performance parameters, such as wind energy utilization coefficient and blade tip speed ratio.

Some researchers have studied the effect of blade icing on the aerodynamic performance of wind turbines through experimental research and numerical simulation. Homola et al. [10] analyzed the influence of icing on the output power of NREL 5 MW wind turbine using BEM theory. It is concluded that icing will cause a 27% loss of wind turbine output power. Barber et al. [11] combined simulation analysis with experimental research. It is concluded that icing can cause a loss of 17% in annual wind turbine power generation. It is believed that the icing near the 5% area of the blade tip has the greatest impact on the output of the unit, which is a key area to be considered for anti-icing and melting ice. Lamraoui et al. [12] studied the effects of environmental parameters on wind turbine blade icing characteristics and power loss through numerical simulation. Studies have shown that the power loss after the blade freezes is mainly located along the blade's span of 0.8, and the maximum power loss can reach 40%. The study of Blasco et al. [13] shows that the wind turbine output power can be achieved by adjusting the pitch angle after icing. Without applying aerodynamic load, adjusting the pitch angle can stabilize the power of the wind turbine and maintain it at the rated level. Oloufemi et al. [14] found that even brief icing can cause significant power loss in stalled wind turbines. However, the wind turbine controlled by the pitch control is relatively less affected.

It can be concluded from the above research: Firstly, most studies on the deterioration of wind turbine performance caused by icing are based on numerical simulations. The numerical simulation will ignore many influencing factors, resulting in a great difference between the simulation results and the test results. Furthermore, it is restricted by the test site and conditions. Experimental research mainly revolves around small wind turbines and blade airfoils. The icing test is carried out under the conditions of indoor temperature control and constant speed. There is a big difference from the wind turbine icing in the natural environment, and the research results are more difficult to apply to engineering practice. In addition, there are few studies on the characterization methods of blade icing degree. Some scholars have proposed to use the leading edge thickness of the blade as a characterization value, which will not be able to establish an organic relationship with the degree of ice accumulation of different airfoil blades.

This paper uses the wind turbine icing test system to conduct icing tests on the blades under natural low temperature environment. During the test, wind speed v , freezing time t and LWC (liquid water content) were used as control variables. The growth characteristics of the ice layer at different positions of the blade were studied. The ratio of the thickness of ice accretion at the leading edge of the blade span length of $0.95R$ to the chord length is proposed as a characteristic value of the wind turbine blade icing degree. By monitoring the changes in wind turbine speed and power during ice accumulation, the effect of icing on the blade tip speed ratio and wind energy utilization coefficient were studied.

2 Ice Coating Test

2.1 Icing Test System and Device

In the natural low temperature environment, the icing test of the rotating blades of the wind turbine has completed. The icing system used in the wind turbine blade icing test is shown in Fig. 1. The icing test system is mainly composed of 4 parts: axial fan, wind turbine, droplet atomization device and signal acquisition device.

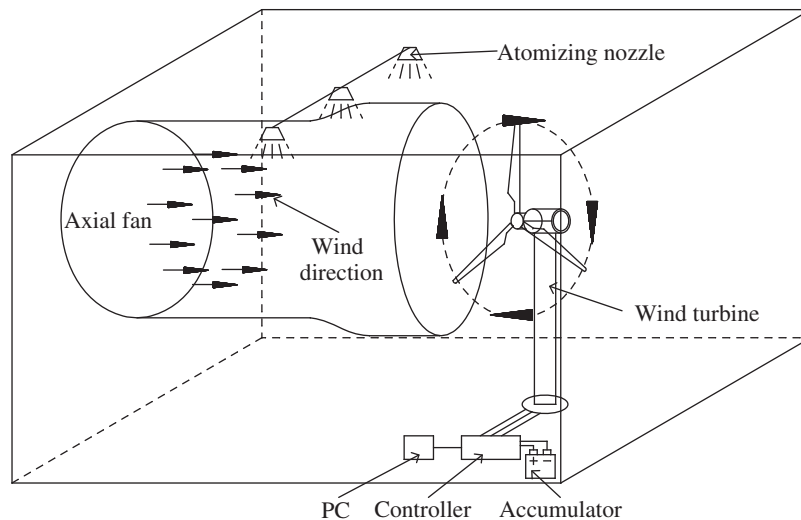


Figure 1: Schematic diagram of wind turbine blade icing test system

The axial fan is shown in Fig. 2a. Its function is to simulate natural wind, adjusting the speed of the axial fan through the frequency conversion controller, in order to achieve the purpose of controlling the wind speed. Its working parameters are: area $1.38 \text{ m} \times 1.3 \text{ m}$, rated voltage 380 V , rated power 1.1 kW , air volume $45000 \text{ m}^3/\text{h}$, adjustable wind speed range $0\text{--}17 \text{ m/s}$. The wind turbine impeller radius R is 1.6 m , and the chord length is between 0.098 m and 0.322 m along the span. The cut-in wind speed is 1.5 m/s ,

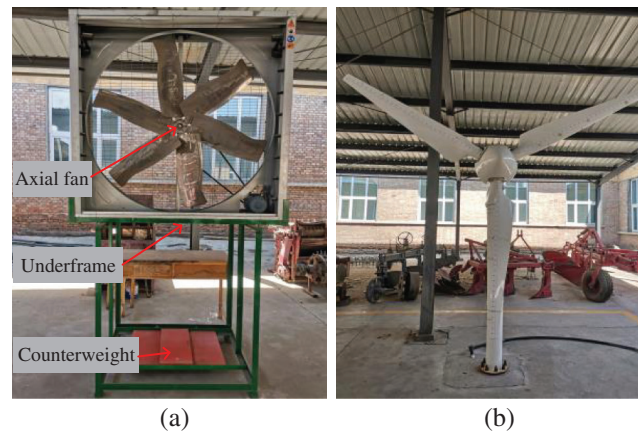


Figure 2: Wind turbine blade icing test device. (a) Axial fan. (b) Wind turbine

and the generator is a three-phase permanent magnet synchronous motor, as shown in Fig. 2b. The droplet atomization device is used to simulate rain and snow weather, and is mainly composed of a high-pressure water pump, three high-pressure atomization nozzles and an overflow valve. The working parameters of the high-pressure water pump are with rated power 15 W, rated pressure 0.6 MPa, and flow rate 1.5 L/min. The atomizing cone angle of the high-pressure atomizing nozzle is 120° , and the atomizing diameter is 0.9 m. The signal acquisition device is mainly composed of 4 parts: PC, controller, battery and load. The controller selects MPPT controller (Maximum Power Point Tracking), and the acquisition frequency is 1 Hz.

2.2 Design of Blade Icing Measurement Point and Definition of Icing Degree

Lamraoui et al. [12] studied the effect of blade icing position on wind turbine output power through simulation, and proposed that the power loss after blade icing is mainly located at the position of $r/R = 0.8-0.95$ along the blade direction; Battisti [15] believes that the maximum thickness of the blade icing is located at the leading edge position of $r/R = 0.9-0.98$ along the blade direction. In order to study the icing at different positions along the direction of blade expansion, the actual situation during the test was combined. In this paper, $0.2R$, $0.6R$ and $0.9R$ are selected as the observation positions of ice accumulation in the blade root, blade middle and blade tip, as shown in Fig. 3a.

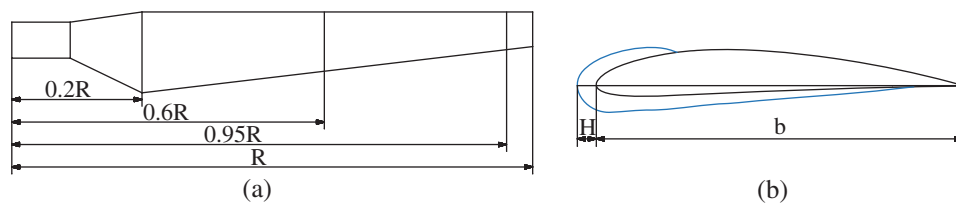


Figure 3: Characterization method of blade icing degree. (a) Blade measuring point design. (b) Airfoil icing schematic

In this paper, the degree of blade icing is defined as: the ratio of the thickness of the ice layer at the leading edge position to the chord length at $0.95R$ along the blade span direction. The airfoil section of the icing blade is shown in Fig. 3b. The calculation method of the degree of icing is shown in Eq. (1):

$$\lambda = \frac{H}{b} \times 100\% \quad (1)$$

In the formula, λ is the degree of ice accumulation, H is the maximum ice thickness of the airfoil, and b is the chord length of the blade.

2.3 Test Method of Blade Icing

During the icing test, Cos-03 high-precision temperature and humidity meter is used to measure the environmental parameters and record the test temperature. This test is operated at a natural low-temperature, the test temperature is -15 to -9°C . In the test, the JRL-FS wind cup anemometer was used to measure and record the wind speed corresponding to different speed of the axial fan. The wind speed used in the test was as follows ($v = 3, 5, 9, 11, 13, 15$ m/s). In the experiment, the freezing time ($t = 5, 10, 20, 30, 60, 90, 120, 150$ min) was selected as the monitoring point.

The axial fan simulates natural wind, blows the super-cooled water droplets generated by the atomizing device to the running wind turbine, and freezes the blades. The variable frequency controller was tested and adjusted to control the speed of the axial fan to achieve the purpose of controlling the wind speed. By changing the number of nozzles, the size of LWC in the atmosphere is adjusted.

After the end of each icing test, the machine is stopped to record the weight of ice accumulation on the blade, and measure the thickness of the ice accumulation on the leading edge of the blade at $0.2R$, $0.6R$ and $0.95R$. When measuring the icing thickness, a Vernier caliper is used to measure each position for 7 times. The maximum and minimum values have been deleted, and 5 valid data are kept for calculating the average. Take the average value as the thickness of the blade icing under the corresponding conditions, and record the ice accumulation of the blade after the test.

2.4 Measurement Method of Wind Turbine Output Parameters

After the icing test is completed, the droplet atomization device is turned off, a signal acquisition device is connected, and the output signal of the wind turbine is measured. The MPPT controller is connected to the wind turbine output port. The output port of MPPT controller is connected to the battery, load, and PC. Each test needs to wait for the wind turbine to rotate smoothly, and then the output signals of the wind turbine current, voltage and speed will be measured and recorded within 5 min, and the average and standard deviation are calculated to be used as the test data of the monitoring point. The computer records the current and voltage signals collected by the controller, and calculates the real-time output power of the wind turbine. In order to improve the reliability of the signal acquisition device, RS485 serial communication is selected as the communication method between the computer and the controller. The test plan is shown in [Tab. 1](#).

Table 1: Test plan

R (m)	LWC ($\text{g}\cdot\text{m}^{-3}$)	MVD (μm)	T ($^\circ\text{C}$)	v (m/s)	t (min)
1.6	0.92	20	-15 to -9	3	5
				5	10
				7	20
				9	30
				11	60
				13	90
				15	120
					150

R is the blade rotation radius, LWC is the Liquid Water Content, MVD (Medium Volume Droplet) is the diameter of the droplet particles, T is the ambient temperature, v is the wind speed, and t is the length of ice accumulation.

3 Results and Discussion

3.1 Icing Test Results

In this paper, the icing test of the working wind turbine was carried out under natural low temperature. By controlling the ice accumulation time t , wind speed v and liquid water content LWC , the ice accumulation distribution of the blade under different parameters is obtained. The icing conditions ($t = 5, 10, 20, 30, 60, 90, 120, 150$ min), $v = 6$ m/s and $LWC = 0.92$ g·m⁻³ were selected as cases for analysis and discussion. The ice thickness of the blades along the wingspan of 0.2R, 0.6R and 0.95R at the leading edge of the blade was measured respectively. The icing thickness test results are shown in Tab. 2. The results of each test have been archived as photos, as shown in Fig. 4.

Table 2: Thickness of ice on the leading edge of the blade

t (min)	0.2R (mm)	0.6R (mm)	0.95R (mm)
5	0.32 ± 0.03	0.60 ± 0.04	0.84 ± 0.02
10	0.58 ± 0.02	1.02 ± 0.04	1.52 ± 0.03
20	1.06 ± 0.03	1.94 ± 0.01	2.78 ± 0.04
30	1.50 ± 0.01	2.80 ± 0.04	4.04 ± 0.03
60	2.92 ± 0.03	5.32 ± 0.07	7.22 ± 0.09
90	4.30 ± 0.13	6.58 ± 0.06	9.18 ± 0.09
120	5.68 ± 0.09	7.82 ± 0.07	10.92 ± 0.10
150	7.04 ± 0.08	9.74 ± 0.10	12.78 ± 0.11

It can be seen from Tab. 2 and Fig. 4 that under the test conditions, the ice accumulation of the wind turbine blades appears translucent and the texture is hard. The icing area is mainly concentrated on the leading edge and windward surface of the blade, the icing on the leeward surface is concentrated near the leading edge of the blade, and the largest ice accumulation position on the airfoil section is on the leading edge of the blade. The thickness of the ice accretion on the blade will increase with the increase of the ice accretion duration, and the amount of ice accretion changes significantly along the blade span. The ice accretion shows the least at 0.2R, followed by 0.6R, and most at 0.95R.

When $t = 5$ min, the icing is mainly concentrated on the leading edge of the blade, and the ice accumulation began to spread from the position of the leading edge of the blade to the windward surface, and no ice adhered to the trailing edge of the blade. When $t = 10$ min, the windward surface of the blade tip was completely covered by ice accumulation, and there was a small amount of ice accumulation in the middle of the blade and the leading edge of the blade root. When $t = 20$ min, the windward side of the blade was completely attached with ice, and the glaze ice first appeared on the windward side of the blade tip. As the experiment progressed, the ice angle of the glaze ice became more apparent, and the glaze ice diffused from the tip of the blade to the middle area of the blade. When the experiment was carried out for 60 min, the obvious glaze ice appeared in the middle of the leaves. Subsequently, the ice angle of glaze ice became more and more obvious. The angle between the growth direction of the ice angle and the leading edge of the blade are mainly concentrated in the range of 18°–62°. Compared with the 0.6R position, the angle between the ice angle at 0.95R position and the leading edge of the blade increased significantly, and no glaze ice appeared in the root area until the end of the experiment. The glaze ice at 0.95R and 0.6R positions at the ice accumulation time ($t = 120$ min) was selected as the observation sample, as shown in Fig. 5.

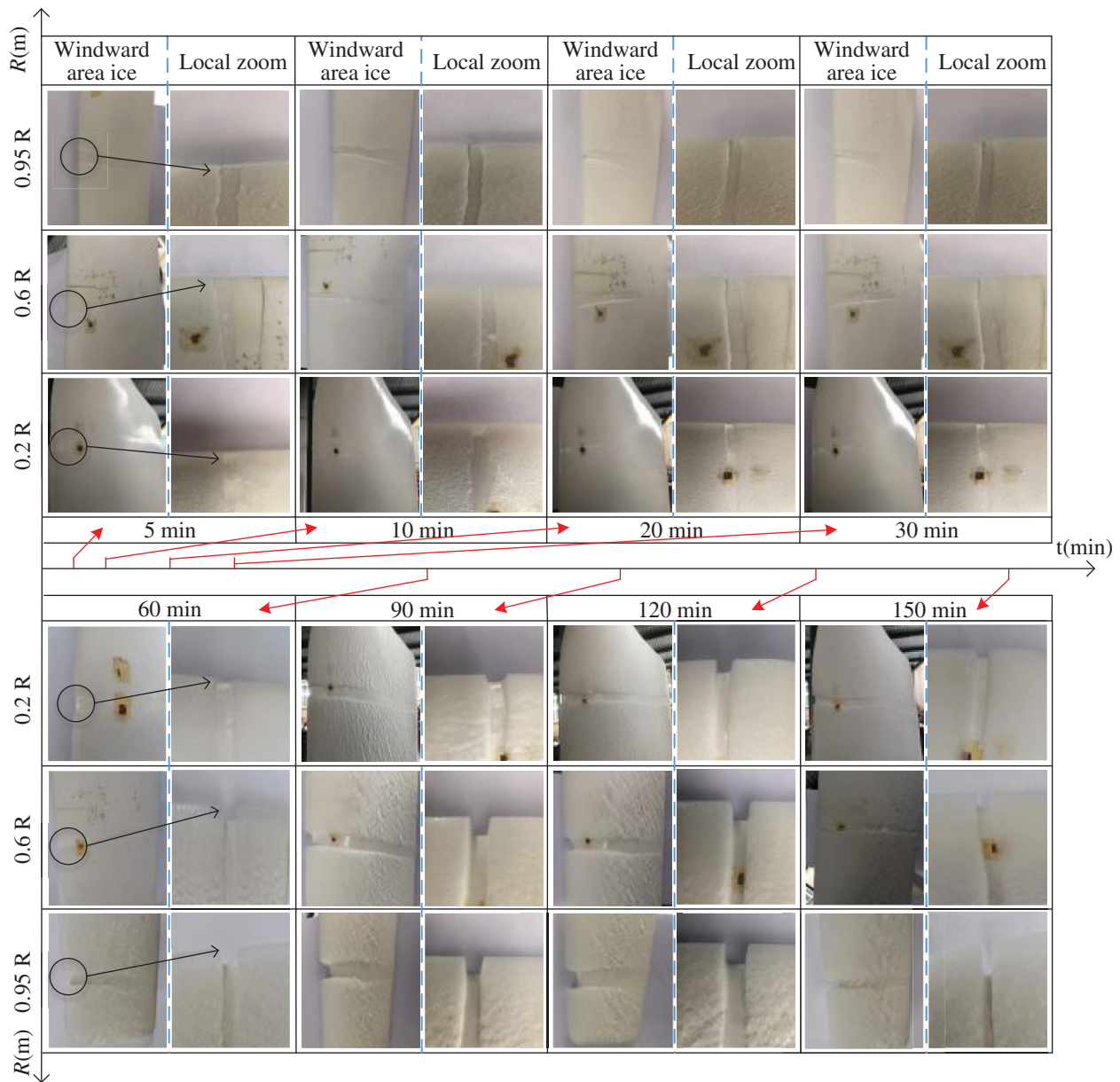


Figure 4: Blade icing test results

Through experimental observation and analysis, the reasons for the above glaze ice are: (1) When the super-cooled water droplets hit the blade rotating at high speed, it mainly hits the position of the leading edge of the blade; (2) The super-cooled water droplet will not freeze immediately when it touches the surface of the blade. It has both radial and tangential motion along the plane of rotation of the blade under the action of inertial and centrifugal forces, as shown in Fig. 6. Under the action of centrifugal force, the super-cooled water droplets have radial movement along the blade span direction, which causes ice accumulation to accumulate at the tip of the blade, resulting in a fast growth rate of ice accumulation at the blade tip. Under the action of inertial force, the super-cooled water droplets move tangentially along the windward surface of the blade, causing the ice accumulation area to spread from the leading

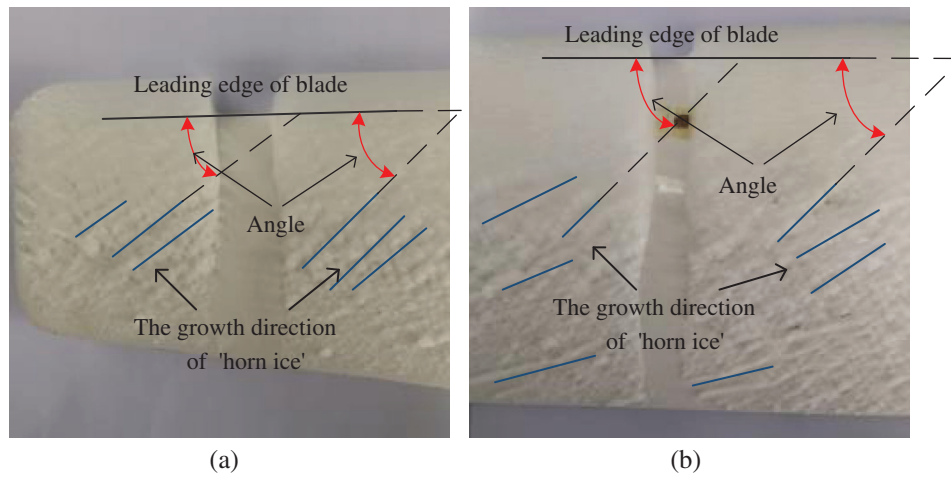


Figure 5: Glaze ice attached to the 0.95R and 0.6R leaves. (a) 0.95R icing state. (b) 0.6R icing state

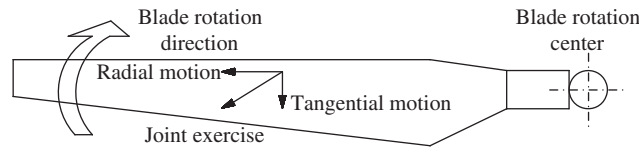


Figure 6: Analysis of the movement of super-cooled water droplets

edge to the trailing edge of the blade. Under the combined force of the two, there is an angle between the growth direction of the ice angle and the leading edge of the blade.

3.2 Analysis of Blade Icing Degree and Icing Thickness Growth Characteristics

The chord length of the blade at the 0.95R position in the blade spreading direction is 102 mm. The icing thickness at the 0.95R position of the blade was measured, and the degree of icing corresponding to different ice accumulation durations was calculated by Eq. (1), as shown in Tab. 3. Fig. 7 shows the growth curve of the blade icing degree. It can be seen from the figure that the growth rate of the blade ice accumulation rate is faster within 60 min, and the growth rate is reduced after 60 min.

Table 3: Icing degree

t (min)	0	5	10	20	30	60	90	120	150
H (mm)	0.00	0.84	1.52	2.78	4.04	7.22	9.18	10.92	12.78
b (mm)	102								
λ	0.00%	0.82%	1.49%	2.73%	3.96%	7.08%	9.00%	10.71%	12.53%

Fig. 8 is a graph of the icing thickness over time at the 0.2R, 0.6R and 0.95R positions of the blade. It can be seen from the figure that the thickness of ice accretion at the 0.95R position of the measuring point increases linearly in the AB segment with the fastest growth rate. Its growth rate can be expressed by the slope of the AB segment, with a growth rate of 12.03%. The ice layer growth rate in section BC gradually decreases. After crossing point C, the thickness of the ice layer shows a steady increase. The growth rate can be expressed by the slope of the CD segment, and the growth rate is 6.00%.

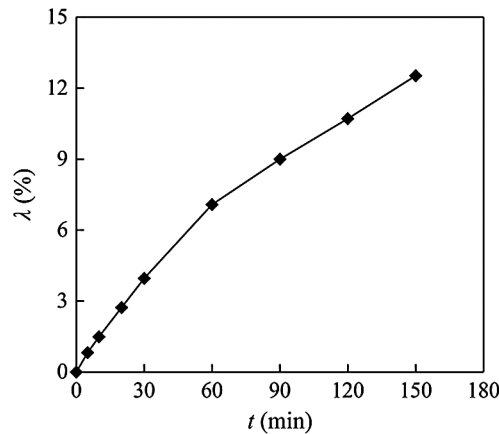


Figure 7: Curve of icing degree

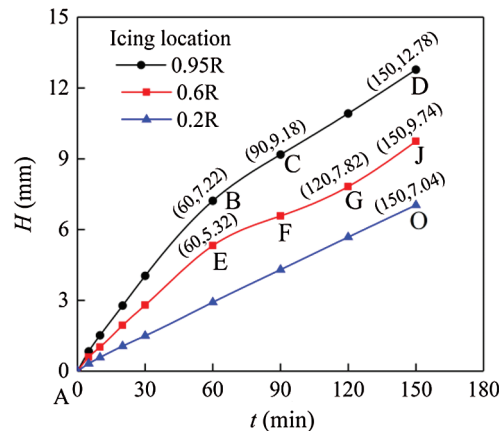


Figure 8: Ice thickness distribution at the 0.2R, 0.6R and 0.95R positions of the blade

The icing thickness at the measuring point of 0.6R is linearly increased in the AE segment, and its growth rate can be expressed by the slope of the AE segment with a growth rate of 8.87%. The growth rate of the EF segment gradually decreases, and then the growth rate of the FG segment increases briefly. After hitting the G point, the GJ growth rate no longer changes, and the growth rate can be represented by the slope of the GJ segment, with a growth rate of 6.40%. During the test, the icing thickness at the measuring point 0.2R increased linearly, and the growth rate was represented by the slope of the AO segment, with a growth rate of 4.69%.

There are two main reasons for the above phenomenon: (1) The wind turbines in the AB and AE sections have high rotation speeds, the centrifugal force of the super-cooled water drops is large, and the radial flow ability is strong, and they gather from the root to the tip of the blade; (2) The linear velocity of the blade tip is large, and the collision efficiency of the super-cooled water droplets is high. Compared with the root portion of the blade, the blade tip can capture more super-cooled water droplets within the same time.

As the degree of ice accumulation continues to increase, the wind turbine load gradually increases, the speed decreases, and the blade tip linear velocity decreases. The speed of the impeller of the wind turbine is reduced, which causes the centrifugal force on the blades of the super-cooled water drops to be reduced, and the radial flow capacity is weakened. And the reduction of the speed will also reduce the collision efficiency of the blade tip. Under the combined effect of the two, the ice growth rate of the EF and BC sections is

reduced. The increase in ice growth rate in the FG section may be due to the decrease in the speed of the wind turbine, which caused the radial flow of super-cooled water droplets near the 0.6R position to the blade tip position weakened, and the super-cooled water droplets quickly attached to form ice coating at 0.6R. As the degree of icing continues to increase, the speed of the wind turbine further decreases, and the radial flow of super-cooled water droplets tends to stop, causing the slopes of the CD and GJ sections to become the same. The 0.2R position is close to the center of rotation of the impeller, and the centrifugal force is the weakest. Therefore, the thickness of icing increases linearly throughout the test, and the slope of the AO segment tends to be a constant value.

3.3 The Effect of the Degree of Icing on the Speed and the Tip Speed Ratio

TSR (tip speed ratio) is an important parameter of wind turbine performance, and its size directly affects the wind energy utilization coefficient. The specific meaning of TSR shows the ratio of blade tip linear velocity to wind velocity, see Eq. (2). Its relationship with the wind turbine speed was converted, as shown in Eq. (3).

$$\varphi = \frac{\omega R}{v} \quad (2)$$

$$\varphi = \frac{\pi n R}{30v} \quad (3)$$

In the formula, ω is the angular velocity; φ is the tip speed ratio; n is the speed of the wind turbine; R is the blade length; v is the wind speed.

It can be seen from Eq. (3) that when the wind turbine blade length R is constant, the size of the TSR is related to the wind turbine speed n and wind speed v . Tab. 4 records the test data of the wind turbine speed under different degrees of icing and the TSR value calculated based on the speed.

Table 4: Changes in speed and blade tip speed ratio

λ	3 (m/s)		5 (m/s)		7 (m/s)		9 (m/s)		11 (m/s)		13 (m/s)		15 (m/s)	
	$n \times 10$	TSR												
0%	28	15.6	40	13.4	54	12.9	66	12.3	82	12.5	96	12.4	108	12.1
0.82%	26	14.5	36	12.1	48	11.5	54	10.0	60	9.1	66	8.5	78	8.7
1.49%	24	13.4	32	10.7	42	10.0	48	8.9	54	8.2	60	7.7	66	7.4
2.73%	22	12.3	28	9.4	36	8.6	42	7.8	48	7.3	54	7.0	66	7.4
3.96%	20	11.2	24	8.0	30	7.2	36	6.7	42	6.4	48	6.2	60	6.7
7.08%	16	8.9	20	6.7	26	6.2	32	6.0	36	5.5	42	5.4	54	6.0
9.00%	12	6.7	18	6.0	24	5.7	30	5.6	36	5.5	40	5.2	48	5.4
10.71%	12	6.7	12	4.0	18	4.3	24	4.5	30	4.6	36	4.6	42	4.7
12.53%	0	0.0	0	0.0	12	2.9	18	3.3	24	3.7	30	3.9	36	4.0

The test results show that at the same wind speed, icing will cause the speed of the wind turbine to decrease, which in turn will cause the change of blade tip speed ratio. According to the test data given in Tab. 4, the relationship between the degree of ice accumulation and the speed and TSR was plotted, as shown in Figs. 9 and 10. It can be seen from Fig. 9 that as the degree of icing increases, the speed of the impeller of the wind turbine decreases. At the beginning of the test, the speed of the impeller

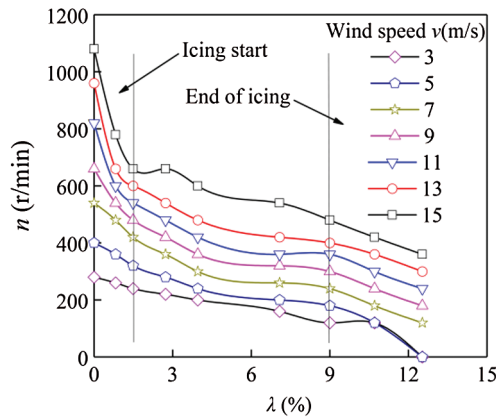


Figure 9: The effect of icing degree on rotating speed

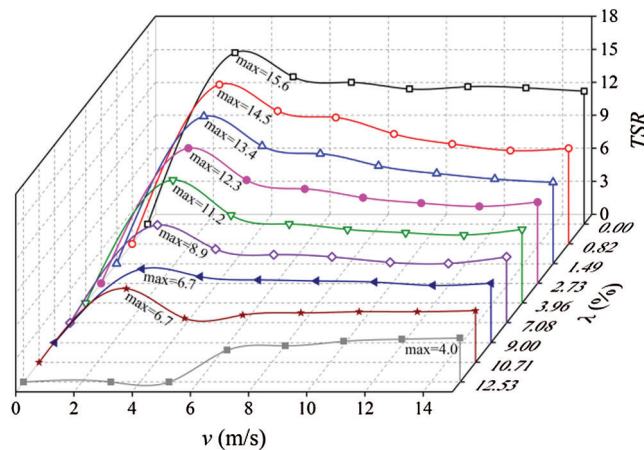


Figure 10: The effect of icing degree on TSR at different wind speeds

decreased most drastically. The speed at the beginning of icing dropped sharply at a rate of 5.56% per minute, and then the rate of decrease slowed down. At the end of the test, the reduction rate of the impeller speed at different wind speeds tends to be the same, and the reduction rate is about 4.32%. The CD segment speed in Fig. 9 drops to 0. The reason for this phenomenon is that when the wind turbine speed is lower than a certain value, the thrust on the shaft is not enough to maintain the rotation of the wind turbine, which will cause the wind turbine to stop.

Fig. 10 shows the trend of tip speed ratio TSR under different icing levels. It can be seen from the figure that as the wind speed v increases, the TSR first increases sharply, then decreases, and finally tends to a constant value. It can be found that the effect of icing on the TSR is most significant in the first three orders, so this article analyzes and discusses the first three orders. When the degree of icing is 0 (clean blade), the maximum tip speed ratio is 15.6. As the degree of icing increases, the tip speed ratio at the same wind speed continues to decrease. When the degree of icing of the blades was 0.82%, 1.49% and 2.73% the maximum tip speed ratio decreased by 7.1%, 14.1% and 21.2% respectively. When the degree of icing is 12.53%, the wind speed is less than 5 m/s and the wind turbine not started. When the wind speed is greater than 5 m/s, the tip speed ratio increases rapidly, and then the TSR tends to reach a stable value of 4.0. The reason for this phenomenon is that as the degree of icing increases, the blade load increases, causing the blade tip speed ratio to decrease. And the increase in the degree of icing will cause the wind turbine to start with a greater cut-in wind speed.

3.4 Effect of Icing Degree on Wind Energy Utilization Coefficient

Wind energy utilization factor C_p is another important parameter of wind turbine performance, which represents the conversion efficiency of wind turbines to convert wind energy into electrical energy. According to Bates theory, the maximum C_p of a wind turbine is 0.593. The specific relationship between it and wind turbine power is shown in Eq. (4):

$$C_p = \frac{P}{0.5\rho\pi R^2 v^3} \quad (4)$$

In the formula, P is power; ρ is atmospheric density; R is wind wheel radius; v is wind speed.

According to the voltage and current signals collected by the controller, the output power of the wind turbine is calculated, as shown in Fig. 11. It can be seen from the test results that with the same wind speed, as the degree of icing increases, the output power of the wind turbine generally shows a downward trend. The loss of output power is most severe at the beginning of icing. Within 5 min before the start of the test, the output power of the wind turbine decreased linearly, and the power loss per minute was about 11.03%. Then the output power of the wind turbine is lost further until the output is close to 0.

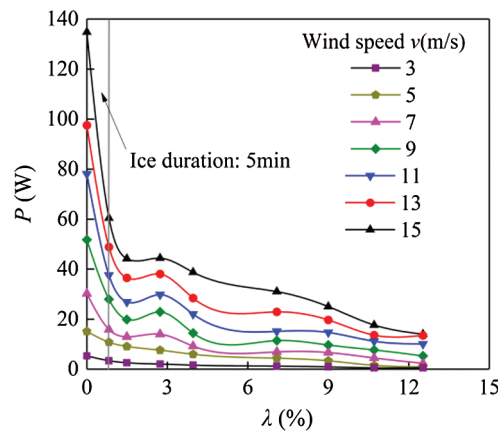


Figure 11: The effect of icing degree on output power

The power data obtained by the experiment is brought into Eq. (4), and the actual wind energy utilization coefficient of the wind turbine is calculated, and the result is given in Fig. 12. It can be seen from the figure that the wind energy utilization coefficient can reach the maximum value when the blade icing degree is 0 (clean blade), and the maximum value of the wind energy utilization coefficient is 0.375.

In the theoretical design of wind turbine blades, it is considered that the wind energy utilization coefficient C_p is a function of the tip speed ratio φ and the pitch angle β , that is $C_p = f(\varphi, \beta)$. The wind energy utilization coefficient C_p can be given by Eq. (5).

$$C_p = (0.44 - 0.0167\beta) \cdot \sin\left[\frac{\pi(\varphi - 3)}{15 - 0.3\beta}\right] - 0.00184(\varphi - 3) \cdot \beta \quad (5)$$

In the formula, φ is the tip speed ratio; β is the pitch angle.

Through MATLAB software, the empirical Eq. (5) is numerically simulated, setting the calculation interval $[0,20]$ of the tip speed ratio φ , and the calculation step as 0.1. The calculation interval of the pitch angle β is $[0,20]$, and the calculation step is 0.5. In the experiment, the pitch angle of the wind

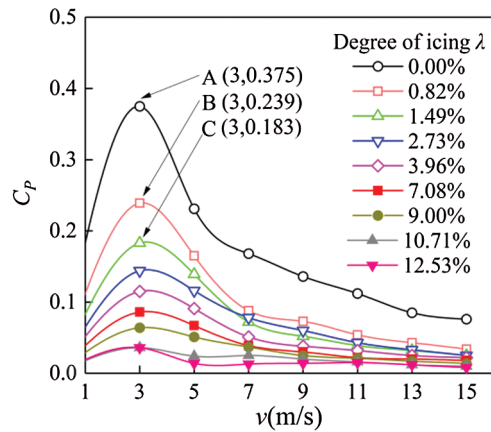


Figure 12: The effect of icing degree on wind energy utilization coefficient

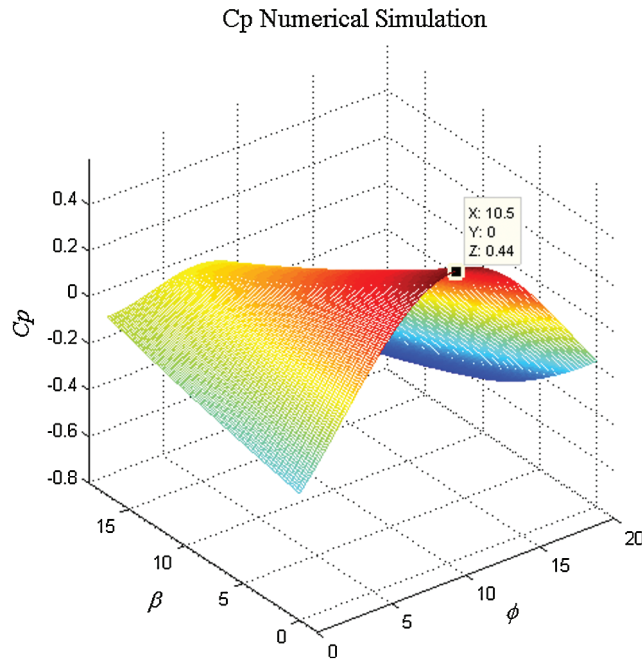


Figure 13: Numerical simulation results of C_P

turbine blade $\beta = 0$, and the change range of the blade tip speed ratio is 0–15.6. The results of the numerical simulation are shown in Fig. 13. From the figure, it can be seen that when the pitch angle $\beta = 0$ and the tip speed ratio $\phi = 10.5$, the maximum value of C_P is obtained. The maximum value of theoretically calculated wind energy utilization coefficient is 0.440.

As can be seen from Fig. 12, within the scope of this study, as the degree of icing increases, the coefficient of wind energy utilization continues to decrease. The effect of icing on the wind energy utilization coefficient C_P is the most severe in the first three orders. Therefore, this article focuses on the first three orders. When the icing degree of the blades is 0.82%, 1.49% and 2.73%, the maximum wind energy utilization coefficient is reduced by 36.3%, 51.2% and 61.6% respectively. Comparing Fig. 12 with Fig. 13, it can be found that the maximum value of the theoretically calculated wind energy utilization coefficient is 0.440, and the maximum wind energy utilization coefficient obtained in the

experiment is 0.375. The reason for this phenomenon may be that, in the actual working process of the wind turbine, there is friction loss in the transmission part. Friction loss will cause the actual power generation of the wind turbine to be lower than the theoretically calculated value. After calculation, the mechanical efficiency of the prototype is about 0.85.

In the actual operation of the wind turbine, due to mechanical efficiency, the actual power generation of the wind turbine is lower than the theoretical calculation value.

4 Conclusions

In this paper, the natural low temperature was used to test the icing of the NACA4412 airfoil wind turbine. An evaluation method of blade icing degree was established. The growth rule of wind turbine blade icing under natural low temperature conditions and the influence of the degree of icing on the wind turbine blade tip speed ratio and wind energy utilization coefficient were studied, and the following conclusions were obtained:

1. Under the test conditions, the icing area is mainly concentrated on the leading edge of the blade and the windward surface. The location of maximum icing is on the leading edge of the blade. The thickness of icing varies significantly along the direction of blade expansion, with the least amount of ice accretion at 0.2R position, followed by 0.6R position, and most at 0.95R position.
2. The icing thickness at the 0.95R position of the blade grows fastest in the early stage of the test. In the early stage of the experiment, it increased linearly, and then the growth rate gradually decreased. At the beginning of the experiment, the thickness of the icing at the 0.6R position of the blade increased linearly. Then the growth rate first decreases and then increases. Throughout the experiment, the icing thickness at the 0.2R position of the blade increased linearly.
3. At a certain wind speed, the speed of the wind turbine decreases as the degree of icing increases. At the beginning of the test, the speed of rotation dropped sharply, and then the speed of decline became slow. Under the influence of the gradual decrease of the impeller speed, the TSR continues to decrease as the blade icing increases.
4. As the degree of icing increases, the output power of the wind turbine gradually decreases. Within 5 min of the start of the test, the output power of the wind turbine decreased linearly. As the degree of icing increases, the wind energy utilization factor of wind turbines continues to decrease. The effect of icing degree on wind turbine output and wind energy utilization coefficient is the most serious in the first three orders.

Acknowledgement: The authors sincerely thank the colleagues in the laboratory during the experiment.

Funding Statement: The author received funding for the “National Natural Science Foundation of China” project (Project Number: 51665052) in this study.

Conflicts of Interest: The authors declare that they have no conflicts of interest to report regarding the present study.

References

1. Wang, Z., Zhu, C. (2017). Numerical simulation for in-cloud icing of three-dimensional wind turbine blades. *Simulation: Transactions of the Society for Modeling and Simulation International*, 94(1), 31–41. DOI 10.1177/0037549717712039.
2. Gao, L., Liu, Y., Zhou, W., Hu, H. (2018). An experimental study on the aerodynamic performance degradation of a wind turbine blade model induced by ice accretion process. *Renewable Energy*, 133, 663–675. DOI 10.1016/j.renene.2018.10.032.

3. Sznajder, J. (2015). Implementation of an Eulerian method of determination of surface water collection efficiency for atmospheric icing problems. *Transactions of the Institute of Aviation*, 238(1), 91–105. DOI 10.5604/05096669.1151313.
4. Shu, L., Liang, J., Hu, Q., Jiang, X., Ren, X. et al. (2017). Study on small wind turbine icing and its performance. *Cold Regions Science & Technology*, 134, 11–19. DOI 10.1016/j.coldregions.2016.11.004.
5. Han, Y., Palacios, J., Schmitz, S. (2012). Scaled ice accretion experiments on a rotating wind turbine blade. *Journal of Wind Engineering & Industrial Aerodynamics*, 109, 55–67. DOI 10.1016/j.jweia.2012.06.001.
6. Mortensen, K. (2008). *CFD simulations of an airfoil with leading edge ice accretion*. Denmark: Technical University of Denmark.
7. Hochart, C., Fortin, G., Perron, J. (2008). Wind turbine performance under icing conditions. *Wind Energy*, 11(4), 319–333. DOI 10.1002/we.258.
8. Wang, X., Bibeau, E. L., Naterer, G. F. (2007). Experimental investigation of energy losses due to icing of a wind turbine. *Challenges of Power Engineering and Environment*, 14, 1143–1147.
9. Pourseif, T., Afzalian, A. (2017). Pitch angle control of wind turbine systems in cold weather conditions using μ , robust controller. *International Journal of Energy and Environmental Engineering*, 8(3), 197–207. DOI 10.1007/s40095-017-0231-y.
10. Homola, M. C., Virk, M. S., Nicklasson, P. J., Sundsbo, P. A. (2012). Performance losses due to ice accretion for a 5 MW wind turbine. *Wind Energy*, 15(3), 379–389. DOI 10.1002/we.477.
11. Barber, S., Wang, Y., Jafari, S., Chokani, N., Abhari, R. S. (2011). The impact of ice formation on wind turbine performance and aerodynamics. *Journal of Solar Energy Engineering*, 133(1), 42–50. DOI 10.1115/1.4003187.
12. Lamraoui, F., Fortin, G., Benoit, R., Perron, J., Masson, C. (2014). Atmospheric icing impact on wind turbine production. *Cold Regions Science and Technology*, 100, 36–49. DOI 10.1016/j.coldregions.2013.12.008.
13. Blasco, P., Palacios, J., Schmitz, S. (2017). Effect of icing roughness on wind turbine power production. *Wind Energy*, 20(4), 601–617. DOI 10.1002/we.2026.
14. Fakorede, O., Feger, Z., Ibrahim, H., Ilinca, A., Perron, J. et al. (2016). Ice protection systems for wind turbines in cold climate: characteristics, comparisons and analysis. *Renewable and Sustainable Energy Reviews*, 65, 662–675. DOI 10.1016/j.rser.2016.06.080.
15. Battisti, L. (2015). *Wind turbines in cold climates*. Switzerland: Springer International Publishing.